EFFECT OF THE NEUTRAL BEAM HEATING ON THE DYNAMICS OF ITER

M. Naguib Aly and H.H. Abou-gabal
Nuclear Engineering Department, Faculty of Engineering,
Alexandria University, Alexandria, Egypt.

ABSTRACT

A point-kinetics model has been used to investigate the effect of the amount of the auxiliary power and the energy of the injected neutral beam on the dynamics of the International Thermonuclear Experimental Reactor (ITER). Four different confinement scaling have been tried. A multigroup slowing down method is followed to consider the finite thermalization time of the fusion fast α-particles and the injected neutral beam particles. The analysis shows the ability of the reactor to approach a steady state operation. An auxiliary heating scenario of 20 MW, 1.3 MeV neutral beam allows a steady state operation without violating the beta limit . The analysis also shows the sensitivity of the reactor dynamics to the confinement scaling. It has also been shown that the reactor power can be increased by increasing the rate of the injected fuel but varying the energy of the injected fuel does not affect the reactor power.

NOMENCLATURE

n_e	electron density, cm^{-3}
n_i	thermal D-T ion density, cm^{-3}
n_α	thermal α-particle density, cm^{-3}
T_i, T_e	ion and electron temperatures, KeV
τ_{Ei}, τ_{Ee}, $\tau_{E\alpha}$	energy confinement time for ions, electrons and α-particles, sec
τ_{pi}, $\tau_{p\alpha}$	particle confinement time for ions and α-particles, sec
V_i	energy of the injected neutral beam, keV
a	minor radius, m
R	major radius, m
A	aspect ratio = R/a
B	confining magnetic field strength, Tesla
q	tokamak safety factor
κ	elongation
R_e	average reflectivity to microwaves of the surfaces facing the plasma
I	plasma current, MA
A_i	isotopic mass number
κ_x	elongation at the x-point
m_D	deuterium mass, gm
m_T	tritium mass, gm
m_n	neutron mass, gm
m_α	α-particle mass, gm

1. INTRODUCTION

Although it is not clear at this time whether the first generation reactors will be pulsed or steady state systems, it is expected that some of them at some point will operate in a steady state mode. For such systems, the question of dynamics is very important.

Bian [1] developed a simplified approach to determine the dynamic and stability properties in a fusion system. His approach is based on the determination of the system transfer functions. He did not consider the slowing down neither of the fusion fast α-particles nor of the injected neutral beam particles. He restricted his analysis to a tokamak-type system that follows a trapped ion scaling law. Oda et al. [2] examined the dynamic behavior and controllability of fast-fission D-T tokamak hybrid reactors. A hybrid reactor is a reactor concept which contains fissionable materials in its blanket surrounding the plasma. He calculated the evolution of plasma/blanket parameters by considering the slowing down of α-particles. Recently, the dynamic behavior of tokamaks have been examined [3-5] in order to study the characteristic thermal instability of the tokamak reactor as well as the effectiveness of different burn control methods to stabilize the thermal fluctuations.

In this paper, we investigate the dynamics of a tokamak reactor by solving the dynamic equations which govern the temporal behavior of the fusion system. The finite thermalization time of the fusion fast α-particles as well as of the injected neutral beam particles is taken into account by applying a mHxtigroup slowing down method. As will be seen, the different terms in the dynamic equations depend nonlinearly on the plasma parameters. In addition, the dynamic behavior of the system is very sensitive to the confinement scaling considered. Section 2 contains the dynamic model of a fusion system as well as the method of solving the time-dependent dynamic equations. Section 3 applies the model to the International Thermonuclear Experimental Reactor (ITER) to investigate the effect of the amount of the auxiliary power and energy of injected fuel on the beta, the output power as well as on the plasma parameters such as density and temperature. The conclusions of this study are contained in Section 4.

2. DYNAMIC MODEL

The dynamic equations of a fusion system with confined plasma are given as [2-4].

$$\frac{dn_i}{dt} = -\frac{n_i}{\tau_{pi}} - \frac{1}{2} n_i^2 <\sigma v> + S_i, \quad (1)$$

$$\frac{dn_\alpha}{dt} = -\frac{n_\alpha}{\tau_{p\alpha}} + S_\alpha, \quad (2)$$

$$\frac{3}{2}\frac{d}{dt}\left(\sum_{j=i,\alpha} n_j T_j\right) = -\sum_{j=i,\alpha} \frac{3}{2}\frac{n_j T_j}{\tau_{Ej}} - W_{\alpha e} + W_{ei} + P_{\alpha i} + P_{aux,i}, \quad (3)$$

$$\frac{3}{2}\frac{d}{dt}(n_e T_e) = -\frac{3}{2}\frac{n_e T_e}{\tau_{Ee}} + W_{\alpha e} - W_{ei} - P_B - P_s + P_{\alpha e} + P_{aux,e} + P_{OH}, \quad (4)$$

In this model, the fusion plasma is described by a mean concentration n_j, and a mean temperature T_j for each species followed in the reactor. In Eqs.(1)-(4),the energy-averaged fusion reaction rate $<\sigma v>$ is given by [6]

$$<\sigma v> = 3.7 * 10^{-12}\, h(T_i) T_i^{-2/3} \exp\left[-\frac{20}{T_i^{1/3}}\right] \text{cm}^3/\text{sec},$$

where

$$h(T_i) = \begin{cases} 1 & \text{if } T_i < 50\,\text{KeV} \\ \left[1 + \left(\frac{T_i}{70}\right)^{1.3}\right]^{-1} & \text{if } T_i = 50-500\,\text{KeV} \end{cases}$$

Figure (1) contains the plot of $<\sigma v>$ versus ion temperature.

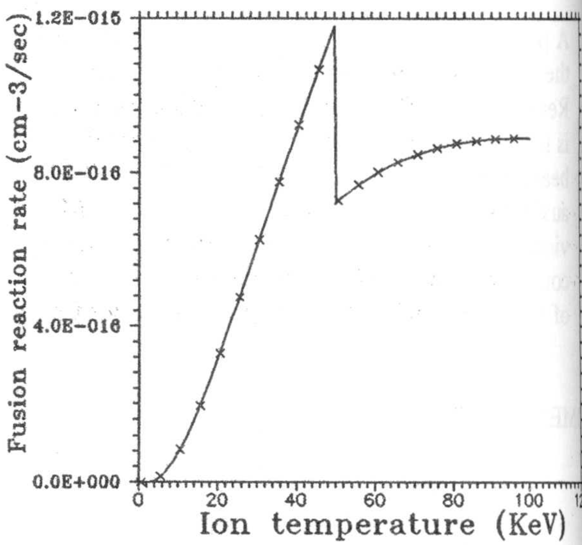

Figure 1. $<\sigma v>$ versus ion temperature.

The rate of energy transfer from the thermal particles to the electrons can be written as [6]

$$W_{\alpha e} = 2.7 * 10^{-12} \frac{n_e n_\alpha (T_\alpha - T_e)}{T_e^{3/2}} \text{KeV/cm}^3\text{sec},$$

while the rate of the energy transfer from thermal ions to electrons can be written as [6]

$$-W_{ei} = W_{ie} = -5.1 * 10^{-13} \frac{n_e n_i (T_e - T_i)}{T_e^{3/2}} \text{KeV/cm}^3$$

The bremsstrahlung loss term is given by [6]

$$P_B = 3.3 * 10^{-15} n_e^2 \bar{z} T_e^{1/2} \text{KeV/cm}^3 \text{sec},$$

where $\bar{z} = \sum_{ions} n_j z_j^2 / \sum_{ions} n_j z_j$ is an average charge number in the plasma.

The synchrotron radiation loss rate takes the following forms [6]

$$P_s = 4.1*10^3\, n_e^{0.5}\, T_e^2 B^{2.5} \left[\frac{1-R_e}{aA}\right]^{0.5} \quad KeV/cm^3\ sec,$$

for $T_e < 50$ KeV, and

$$P_s = 70\, n_e^{0.5}\, T_e^{2.8}\, B^{2.5} \left[\frac{1-R_e}{aA}\right]^{0.5} \quad KeV/cm^3\ sec,$$

for $T_e > 50$ KeV.

The ohmic heating term is given by $<\eta\, j^2>$ [5,7] KeV/cm^3 sec where η is the Spitzer resistivity.

The different particle and energy confinement times will be discussed in Section 3.

The terms $P_{\alpha i}$ and $P_{\alpha e}$ are the α-particle slowing down power density on ions and electrons respectively. They are calculated taking into account the finite thermalization time of the fusion born α-particles. Neglecting the loss of fast α-particles during slowing down, dispersion in energy space and interactions between fast α-particles, the slowing down equation for fast α-particles can be written as [2]

$$\frac{\partial}{\partial t} n_\alpha(E,t) = S_\alpha(E,t) + \frac{\partial}{\partial E}\left[\sum_\beta \left|\frac{dE}{dt}\right\rangle_{\alpha,\beta} (E,t)\, n_\alpha(E,t)\right], \quad (5)$$

where $n_\alpha(E,t)$ is the energy distribution function of fast α-particles and $\left|\frac{dE}{dt}\right\rangle_{\alpha,\beta}(E,t)$ the average energy loss per unit time [8-10] on plasma species β.

The α-particle source distribution, $S_\alpha(E,t)$, is taken as [11]

$$S_\alpha(E,t) = \frac{n_i^2}{4 m_\alpha v_o}\sqrt{\frac{\beta_M}{\pi}} <\sigma v> \exp\left[-\beta_M\left(\sqrt{\frac{2E}{m_\alpha}} - v_o\right)^2\right],$$

where $\beta_M = \dfrac{m_D + m_T}{2kT_i}$ and $V_o = \sqrt{\dfrac{2m_n}{m_\alpha(m_\alpha + m_n)} Q}$ with Q equal to 17.58 MeV. Integrating Eq.(5) in the interval $E_{g+1} \le E \le E_g$, we obtain the following multigroup slowing down equations

$$\frac{dn_\alpha^g}{dt} = S_\alpha^g + \sum_\beta \left[\frac{n_\alpha^{g-1}}{\tau_{\alpha,\beta}^{g-1\to g}} - \frac{n_\alpha^g}{\tau_{\alpha,\beta}^{g\to g+1}}\right],$$

where n_α^g is the density of α-particles in group g (g=1,2,..., G) and S_α^g their source. The quantity $\tau_{\alpha,\beta}^{g\to g+1}$ is defined by [2]

$$\frac{1}{\tau_{\alpha,\beta}^{g\to g+1}} = \frac{1}{n_\alpha^g}\left|\frac{dE}{dt}\right\rangle_{\alpha,\beta} (E_{g+1},t)\, n_\alpha(E_{g+1},t).$$

Using the multigroup quantities, we can express the source of thermalized α-particles and slowing-down power densities as follows:

$$S_\alpha = \sum_\beta n_\alpha^G(t)/\tau_{\alpha,\beta}^{G\to BG} \quad cm^{-3}sec^{-1},$$

$$P_\alpha^i = \sum_{\beta\neq e}\sum_g (\tilde{E}_g - \tilde{E}_{g+1}) n_\alpha^g(t)/\tau_{\alpha,\beta}^{g\to g+1} \quad KeV/cm^3 sec,$$

$$P_\alpha^e = \sum_g (\tilde{E}_g - \tilde{E}_{g+1}) n_\alpha^g(t)/\tau_{\alpha,e}^{g\to g+1} \quad KeV/cm^3 sec,$$

where $\tilde{E}_g$ is the arithmetic mean energy of the group g. The group G is the lowest energy group and BG=G+1 is the background ion population.

The auxiliary power term P_{aux} is assumed to be supplied by high energy neutral beams and therefore is calculated taking into account the finite thermalization time of the fast ions. A treatment similar to that of the slowing down of the fast fusion α-particles is followed to obtain the power imparted to the electrons and the ions, $P_{aux,e}$ and $P_{aux,i}$ respectively, as well as the source of the thermal D-T ions, S_i.

To preserve the quasineutrality property of the plasma, the electron density is given by

$$n_e(t) = \sum_{\beta\neq e}\left\{z_\beta n_\beta(t) + \sum_g z_\beta n_\beta^g(t)\right\}.$$

Impurities are ignored in this model.

Eqs. (1)- (4) are a set of simultaneous nonlinear first order differential equations which can be integrated numerically to give the time dependence of the plasma parameters (n_i, n_α, T_i, and T_e). In this work, the numerical integration was performed using Runge-Kutta method [12].

Released in each D-T reaction are a 3.5 MeV α-particle which is confined by the magnetic field and a 14.1 MeV neutron which escapes from the plasma and is absorbed in the neutron blanket. Since the α-particles are thermalized inside the reactor core and neglecting the energy multiplication obtained from breeding tritium in the neutron blanket, we can write the reactor power output as

$$P_n = \frac{1}{4} n_i^2 < \sigma v > Q_n V,$$

where $V = 2\,\pi^2\, a^3\, A\, \kappa$ is the plasma volume and $Q_n = 14.1$ MeV.

Table 1. ITER parameters.

B = 4.85 Tesla	a = 2.15 m
A = 2.79	q = 3.1
R_e = 90 %	D-T fuel

3. RESULTS AND DISCUSSION

The model has been applied to the International Thermonuclear Experimental Reactor (ITER) [13-15]. In this work, we adopt the physics phase parameters which are summarized in Table (1). As auxiliary heating a scenario of 75 MW, 1.3 MeV neutral beam was proposed. For the confinement laws, we used four different scaling which are:

1. ITER(89) L-mode power law confinement scaling

$$\tau_E^{ITER\,89-p} = 0.048\, I^{0.85} R^{1.2} a^{0.3} \bar{n}_{20}^{-0.1} B^{0.2} (A_i \kappa_x / P)^{0.5} \text{sec}.$$

2. ITER(89) L-mode off-set linear confinement scaling

$$\tau_E^{ITER\,89-OL} = 0.064\, I^{0.8} R^{1.6} a^{0.6} \bar{n}_{20}^{-0.6} B^{0.35} A_i^{0.2} \kappa_x^{0.5} / P + 0.04\, I^{0.5} R^{0.3} a^{0.8} A_i^{0.5} \kappa_x^{0.6} \text{sec}.$$

3. ITER ELM-free H-mode confinement scaling

$$\tau_E^{ITER90-H}(\text{ELM-free}) = 0.064\, I^{0.87} R^{1.81} a^{0.13} \bar{n}_{20}^{-0.09} B^{0.15} A_i^{0.5} \kappa_x^{0.36} P^{-0.51} \text{se}$$

4. ITER ELMy H-mode confinement scaling

$$\tau_E(\text{ELMy H-mode}) \sim 0.75\, \tau_E(\text{ELM free H-mode})$$

where P is the net heating power in MW, defined as $P \approx P_\alpha + P_{aux} + P_{OH}V - P_{rad}$, $\bar{n}_{20}$ is the electr density in 10^{20} m^{-3}. In the calculations, I, A_i and are set equal to 22 MA, 2.5 and 2.22 respectively. F each one of the above confinement scaling, $\tau_{p\alpha}$ and are set equal to 10 τ_E while τ_{Ei}, τ_{Ee} and $\tau_{E\alpha}$ are s equal to τ_E.

The simulation starts at an operating point within th range of values proposed for ITER [13-15] namely $T_i = T_e = 10$ KeV, $n_e = 7.5*10^{13}$ cm^{-3}, n_i = 6.7 10^{13} cm^{-3} and $n_\alpha = 3.75*10^{12}$ cm^{-3}, this correspon to a thermal α-particle concentration n_α/n_e = 5%. group structure, consisting of 10 groups divided in equal energy width above $E_c = 3\, T_i$ up to 6 MeV f the fast fusion α-particles and up to V_i for the injecte neutral beam, is adopted in the multigroup slowin down method.

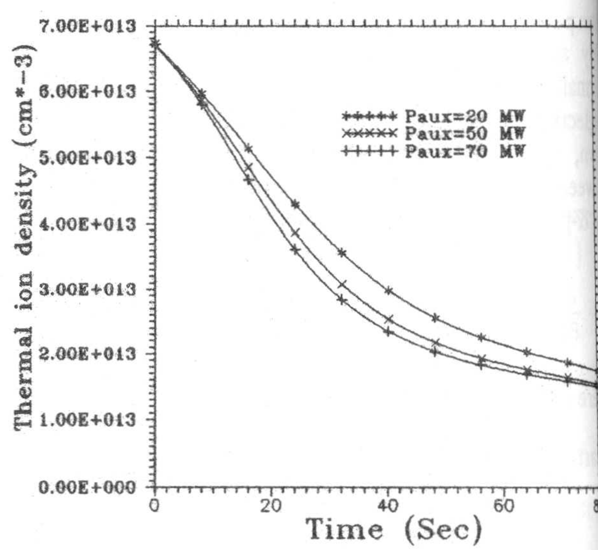

Figure 2. Thermal ion density versus time for differen values of P_{aux}.

The value of the auxiliary power, P_{aux}, has bee perturbed keeping V_i equal to 1.3 MeV. The plasm parameters as well as the reactor power have bee plotted versus time for a period of 80 sec. These plot are shown in Figures (2-7) for the ELM-free H-mod confinement scaling. The figures show that the reacto power and the plasma parameters tend to approac steady state within this period of 80 sec. As can b expected, increasing P_{aux} leads to an increase in the io and the electron temperatures. Figure (2) shows decrease in the thermal D-T ion density as P_{aux} increases. This behavior can be explained by th dependence of $<\sigma v>$ on T_i. In the ion temperatur range considered, $<\sigma v>$ increases with T_i leading to an increase in the fusion rate and subsequently in the rate of loss of the D-T thermal ions. In contradiction, higher fusion rate means higher production of alpha particles. This explains the increase of the α-particle density with P_{aux} observed in Figure (3).

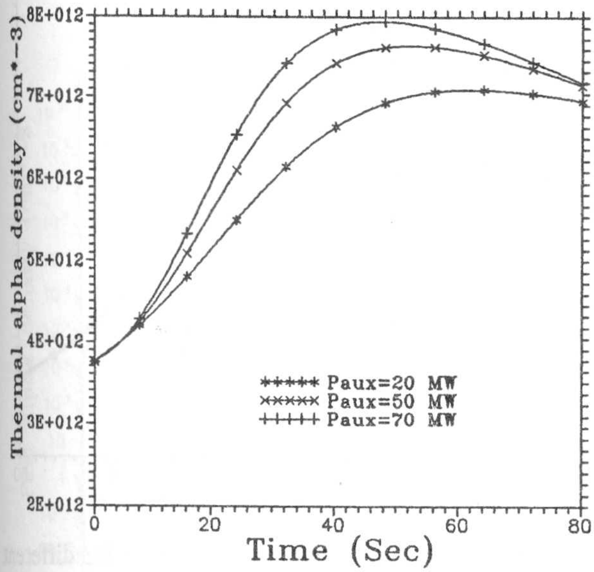

Figure 3. Thermal α-particle density versus time for different values of P_{aux}.

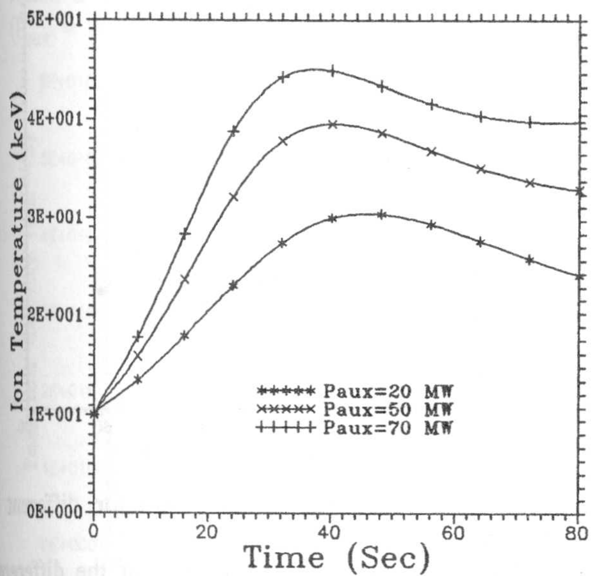

Figure 4. Ion temperature versus time for different values of P_{aux}.

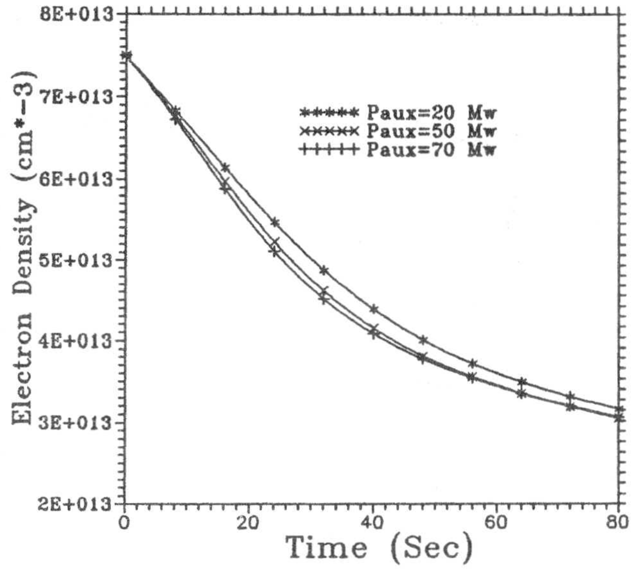

Figure 5. Electron density versus time for different values of P_{aux}.

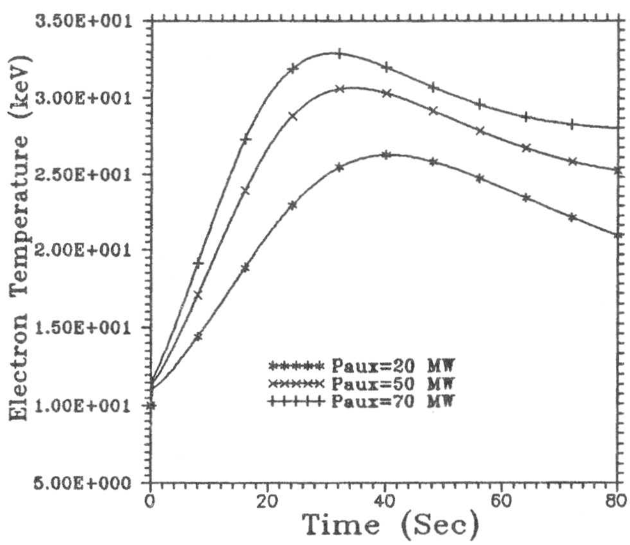

Figure 6. Electron temperature versus time for different values of P_{aux}.

The peak observed in the reactor power, P_n, in Figure (7) can be explained by the contradicting behaviors of n_i and T_i shown in Figures (2) and (4) respectively. As T_i increases with time, the fusion rate increases leading to an increase in P_n but the observed decrease in n_i with time causes P_n to decrease. Up to about 20 sec, the effect of T_i dominates and P_n increases while the effect of n_i dominates after that causing the peak to appear. In Figure (8), the total beta ($\beta_{total}=\beta_{thermal}+\beta_{fast}$) is plotted versus time for different values of P_{aux}.

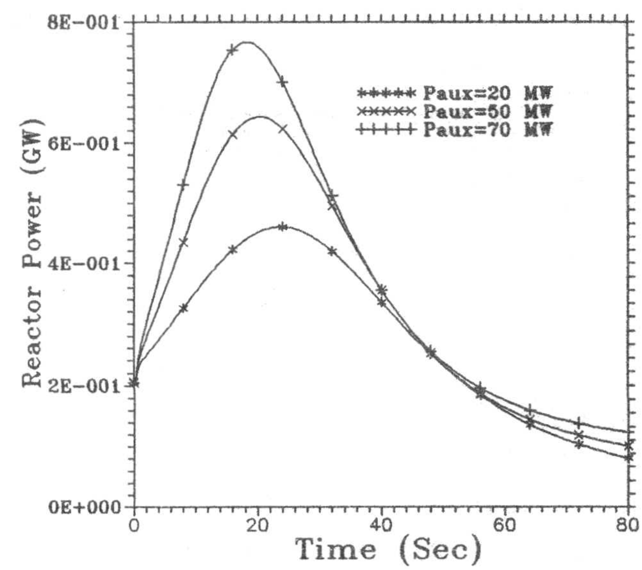

Figure 7. Reactor power versus time for different values of P_{aux} (V_i = 1.3 MeV).

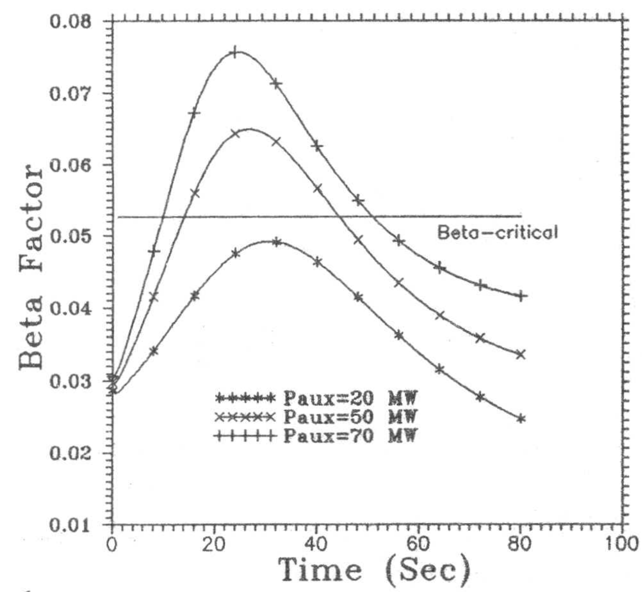

Figure 8. Total beta versus time for different values of P_{aux}.

Also shown on the same plot is the Troyon beta limit curve (β_{crit} = 2.5 I/aB) [4]. It can be seen that the decrease of P_{aux} postpones the violation of the beta limit and at P_{aux} = 20 MW, the total beta does not exceed this limit at all.

Figure (9) and (10) show the time dependence of the reactor power and the total beta for different values of V_i respectively keeping P_{aux} equal to 20 MW. It can observed that P_n and β_{total} are not sensitive to the va of V_i. This means that the dynamic of ITER is affec mostly by the rate of injection of the neutral be particles not by the energy of the particles.

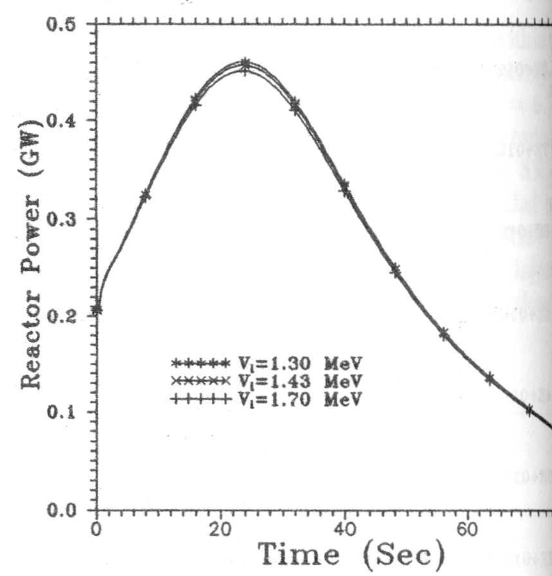

Figure 9. Reactor power versus time for differe values of V_i (P_{aux} = 20 MW).

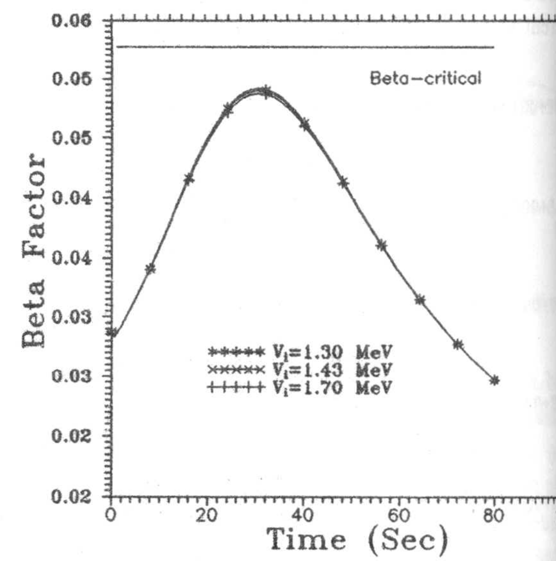

Figure 10. Total beta versus time for differe values of V_i.

The time evolution of the density of the diffe energy groups of the fast fusion α-particles and injected fast D-T ions is shown in Figure (11) and respectively. P_{aux} and V_i are set equal to 20 MW 1.3 MeV respectively. In both cases, group 1 refe the highest energy group. In spite of the continuous feeding of the fast ions in group 1, Figure (12) shows that the densities of the fast ions in the other groups except group 10 are always higher than the density of the ions in group 1. This can be explained by fast thermalization times due to collisions with electrons, thermal D-T ions and thermal α-particles.

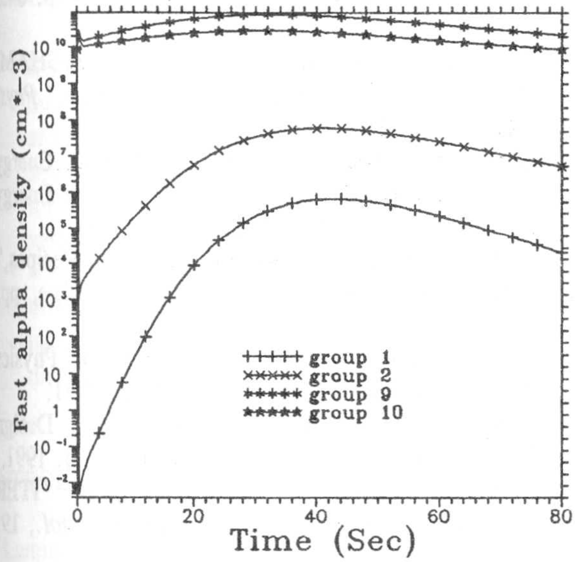

Figure 11. Time variation of the density of the fast fusion α- particles in the different energy groups (P_{aux} = 20 MW, V_i = 1.3 MeV).

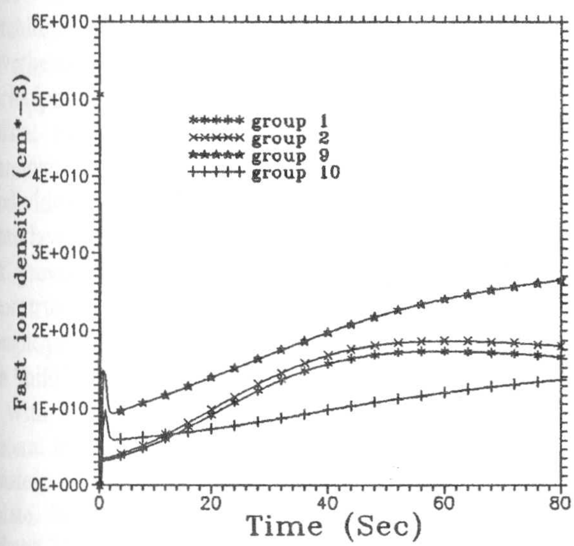

Figure 12. Time variation of the density of the fast D-T ions in the different energy groups (P_{aux} = 20 MW, V_i = 1.3 MeV).

Figure (13) presents the time variation of the reactor power for the different energy confinement scaling considered taking P_{aux} and V_i equal to 20 MW and 1.3 MeV respectively. As can be expected, P_n depends on the scaling considered. The interruption of the curves corresponding to the L-mode scaling indicates the termination of the discharge at this time.

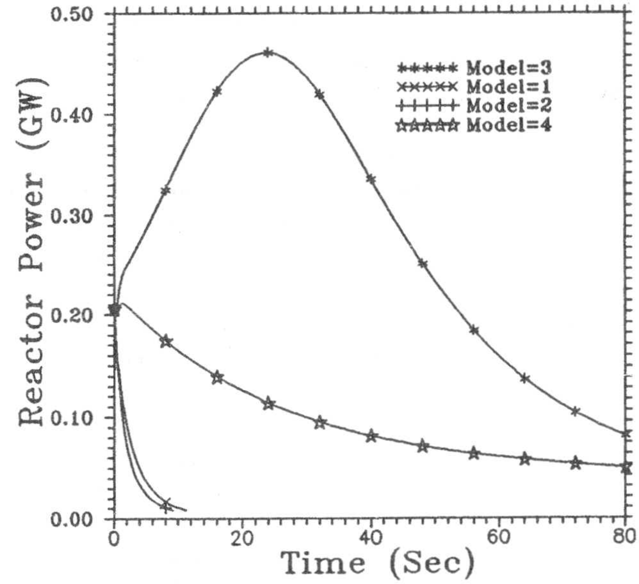

Figure 13. Reactor power versus time for different ITER confinement scaling (P_{aux} = 20 MW, V_i = 1.3 MeV).

4. CONCLUSIONS

The dynamic behavior of ITER has been studied using a point-kinetics model. A multigroup slowing down method has been used to treat the thermalization of the fast fusion α-particles and the injected neutral beam particles. A simulation of the plasma parameters and the reactor power for a period of 80 seconds shows that operation in a steady state mode can be achieved as long as the beta limit is not violated. An auxiliary heating scenario of 20 MW, 1.3 MeV neutral beam can achieve this task. It shows also that the dynamics of ITER depend strongly on the form of the confinement scaling considered as well as on the behavior of $<\sigma v>$ with the ion temperature. It has also been found that the reactor power can be increased by increasing the rate of the injected fuel but is insensitive to the energy of the injected fuel.

REFERENCES

[1] S. BIAN, "Dynamic Analysis of a Fusion System Using the System Transfer Function," *Nucl. Technol.*, **45**, 244, 1979.

[2] A. ODA, Y. NAKAO, K. KPUDO, and M. OHTA, "Dynamic Characteristics and Controllability of Fusion-Fission Hybrid Reactor Systems," *Kerntechnik*, **51**, 186, 1987.

[3] S.K. HO and MAX E. FENSTERMACHER, "Thermally Stable Operation of Engineering Test Reactor Tokamaks," *Fusion Technol.*, **16**, 185, 1989.

[4] JOHN MANDREKAS and W.M. STACEY, Jr., "Evaluation of Different Control Methods for the Thermal Stability of the International Thermonuclear Experimental Reactor," *Fusion Technol.*, **19**, 57, 1991.

[5] GEORGE H. MILEY and V. VARADARAJAN, "On Self-Tuning Control of Tokamak Thermokinetics," *Fusion Technol.*, **22**, 425, 1992.

[6] T. KAMMASH, "Fusion Reactor Physics," Ann arbor science publishers, Inc., Michigan, pp. 203-230 (1975).

[7] N.A. UCKAN, "Relative Merits of Size,Field, and Current on Ignited Tokamak Performance," *Fusion Technol.*, **14**, 299, 1988.

[8] N.A. UCKAN et al., "Influence of Fast Alpha Diffusion and Thermal Alpha Buildup on Tokamak Reactor Performance," *Fusion Technol.*, **13**, 411, 1988.

[9] J.D. CALLEN et al., "Neutral Beam Injection into Tokamaks," Proc. Conf. Plasma Physics and Controlled Nuclear Fusion Research, Tokyo, Japan, November 11-15, 1974, p. 645, 1975.

[10] S.T. BUTLER and M.J. BUCKINGHAM, "Energy Loss of a Fast Ion in a Plasma," *Phys. Rev.*, **126**, 1, 1962.

[11] G. LEHNER, "Reaction Rates and Energy Spectra for Nuclear Reactions in High Energy Plasmas," *Z. Physik*, **232**, 174, 1970.

[12] W.H. Press et al., "Numerical Recipes," Cambridge University Press, Cambridge, pp. 547-577, 1989.

[13] N.A. Uckan and D.E. Post, "ITER Physics Basis," *Fusion Technol.*, **19**, 1411, 1991.

[14] N.A. Uckan et al., "ITER Physics Design Guidelines," *Fusion Technol.*, **19**, 1493, 1991.

[15] N.A. Uckan and J.T. Hogan, "ITER Confinement Capability," *Fusion Technol.*, **19**, 1499, 1991.